Structure
Article

Structural Basis for Specific Recognition of Reelin by Its Receptors

Norihisa Yasui,[1] Terukazu Nogi,[1] and Junichi Takagi[1,*]
[1]Laboratory of Protein Synthesis and Expression, Institute for Protein Research, Osaka University, 3-2 Yamadaoka, Suita, Osaka 565-0871, Japan
*Correspondence: takagi@protein.osaka-u.ac.jp
DOI 10.1016/j.str.2010.01.010

SUMMARY

Apolipoprotein E receptor 2 (ApoER2) and very-low-density lipoprotein receptor, members of the low-density lipoprotein receptor (LDLR) protein family, function as neuronal receptors for a secreted glycoprotein reelin during brain development. In both receptors, the first LDLR class A (LA1) module is sufficient to bind reelin. Analysis of a 2.6 Å crystal structure of the reelin receptor-binding fragment in complex with the LA1 of ApoER2 revealed that Lys2467 of reelin is recognized by both a conserved Trp residue and calcium-coordinating acidic residues from LA1, which together with Lys2360 plays a critical role in the interaction. This "double-Lys" recognition mode is, in fact, shared among other LDLR family proteins in ligand binding. The interface between reelin and LA1 covers a small surface area of ~350 Å^2 on each side, which ensures a stable complex formation under physiological conditions. An examination of structure-guided mutagenesis on interface residues revealed key features of this interaction.

INTRODUCTION

The low-density lipoprotein receptor (LDLR) family of proteins comprises a class of cell-surface type I receptors that share structural features with the endocytotic receptor LDLR. These receptors play essential roles in the cellular uptake of various extracellular ligands, as well as in cellular signaling events implicated in the regulation of neuronal development and tissue morphogenesis (Herz and Bock, 2002). Two closely related members of this family, apolipoprotein E receptor 2 (ApoER2) and very-low-density lipoprotein receptor (VLDLR), function as receptors for a secreted glycoprotein reelin, which plays a critical role in the formation of the mammalian six-layered neocortex (Tissir and Goffinet, 2003). Reelin binding to the extracellular region of ApoER2 or to VLDLR on neurons is believed to initiate the cellular signaling response, resulting in Src family kinase (Src and Fyn)-mediated tyrosine phosphorylation of disabled-1 (Dab1) protein, an intracellular adaptor protein associated with the NPXY sequence in the cytoplasmic tails of ApoER2 and VLDLR. In fact, mice with genetic deficiencies of reelin (Tissir and Goffinet, 2003), ApoER2 plus VLDLR (Trommsdorff et al., 1999), Dab1 (Howell et al., 1997; Sheldon et al., 1997), or Src plus Fyn (Kuo et al., 2005) all exhibit indistinguishable phenotypes including ataxia, cortical layer inversion, and abnormal neuronal positioning patterns. The extracellular regions of reelin receptors consist of three types of protein modules that are commonly present in LDLR family proteins: LDLR class A (LA), epidermal growth factor (EGF), and YWTD β-propeller modules (Kim et al., 1996; Sakai et al., 1994). The LA module is a small protein module (~40 amino acids, usually occurring as a 3–8 concatenation) that has three disulfide bonds and a calcium-binding site formed by highly conserved acidic amino acid residues (Blacklow, 2007). It has been reported that reelin receptors recognize reelin protein through their LA modules (Koch et al., 2002), whereas the exact roles played by the YWTD β-propeller domain and EGF modules remain unknown. The reelin-binding region within ApoER2 was initially mapped to the N-terminal three modules (LA1–3) by Andersen et al. (2003), and then further narrowed down to the first LA module (LA1) using deletion fragments (Yasui et al., 2007). The exact location of the reelin-binding site within the eight LA modules in VLDLR has yet to be reported.

Reelin protein consists of the following components: a signal sequence, a region similar to F-spondin (F-spondin-like domain), a unique region, and eight tandem repeats of 350–390 amino acid residues termed "reelin repeat" (D'Arcangelo et al., 1995; Ichihara et al., 2001). Each reelin repeat is comprised of a central EGF module flanked by subrepeats A and B. Crystal structures of the third repeat (R3) and the tandem R5-6 fragments revealed that two subrepeats directly contact each other despite intervention by the EGF motif, thereby resulting in a compact horseshoe-like structure (Nogi et al., 2006; Yasui et al., 2007). Each subrepeat assumes a β-jelly-roll fold generally known as a carbohydrate-binding domain fold, where 11 β strands form two antiparallel β sheets (Nogi et al., 2006).

Under physiological conditions, reelin is specifically cleaved at two sites located between R2 and R3 and between R6 and R7 by certain metalloprotease activity (Kohno et al., 2009; Lambert de Rouvroit et al., 1999). The resultant central fragment of reelin (R3–6) can bind to receptors and retains its biological activity (Jossin et al., 2003, 2004). The physiological importance of the R3–6 fragment was further highlighted by experiments using cultured brain slices (Jossin et al., 2007).

Previously, we narrowed down the receptor-binding region to the last half of R3–6 (i.e., R5-6) (Yasui et al., 2007). This fragment showed direct binding to the LA module segment of receptors and was capable of inducing the phosphorylation of Dab1 in cultured neurons. Furthermore, a 2.0 Å resolution crystal

 ©2010 Elsevier Ltd All rights reserved

structure of R5-6 enabled us to perform structure-guided mutational analyses, leading to identification of the critical residues (Lys2360 and Lys2467 located in R6) used for receptor binding (Yasui et al., 2007).

In many cases, LDLR family proteins recognize their ligand through their LA module region, which generally contains multiple concatenated modules. To date, several crystal structures of the LA module fragments from LDLR family proteins in complex with their ligand proteins have been reported (Fisher et al., 2004; Rudenko et al., 2002; Verdaguer et al., 2004). In all cases, specific Lys residues of ligand are recognized by LA modules through a common mechanism whereby they are surrounded by conserved aromatic residues and calcium-coordinating acidic residues of LA modules (Fisher et al., 2004). Thus, involvement of reelin lysine residues in receptor binding strongly suggests that the reelin recognition carried out by the receptors is accomplished via a mechanism similar to that used by other LDLR family proteins (Yasui et al., 2007). In order to understand the specific recognition mechanisms used by reelin receptors at an atomic level, we determined the crystal structure of a complex between reelin R5-6 and LA1 of ApoER2.

RESULTS

Recognition of Reelin by a Single LA Module Segment within the Receptors

Previously, we reported that the LA1 module of ApoER2 is both necessary and sufficient for binding to the R5-6 fragment of reelin. It is possible, however, that neighboring modules (i.e., LA2 and/or LA3) also contribute favorably to the binding process, as suggested by Andersen et al. (2003). We therefore prepared recombinant ApoER2 LA1 module fragments with one or more module extensions and compared their binding affinities toward reelin R5-6 using surface plasmon resonance (SPR). As shown in Figure 1, steady-state analysis of the binding isotherms reveals that the two-module receptor fragment (LA12) has a 5-fold higher affinity than LA1 (14 nM versus 73 nM). However, the affinity of the three-module fragment (LA123) was 2-fold lower than LA12, suggesting that the effect of the LA2/LA3 addition on the affinity is of an indirect nature. We also performed isothermal titration calorimetry analysis on the interaction of LA1 or LA12 with R5-6 (see Figure S1 available online). The affinity values were roughly in the same range as that obtained with SPR, albeit with a less pronounced difference between LA1 and LA12 (98 nM for LA1 and 57 nM for LA12), thus running counter to the idea that LA2 binds directly to R5-6. We next tried to determine the reelin-binding region within the second reelin receptor VLDLR. In our previous study, we showed that VLDLR shares the same binding specificity with the primary receptor ApoER2 in that it requires the R5-6 region of reelin, especially the Lys2467. Various numbers of LA modules from human VLDLR (which contains eight LA modules) were fused to human growth hormone (hGH) and the resultant fusion proteins were evaluated for binding to reelin R5-6 in pull-down assays using anti-hGH antibody beads. As shown in Figure 2A, any fragment containing the first LA module, including that comprised of LA1 alone, could bind R5-6, whereas those fragments lacking LA1 did not show detectable binding. This result not only establishes that VLDLR also uses the LA1 module located at the most N-terminal reach

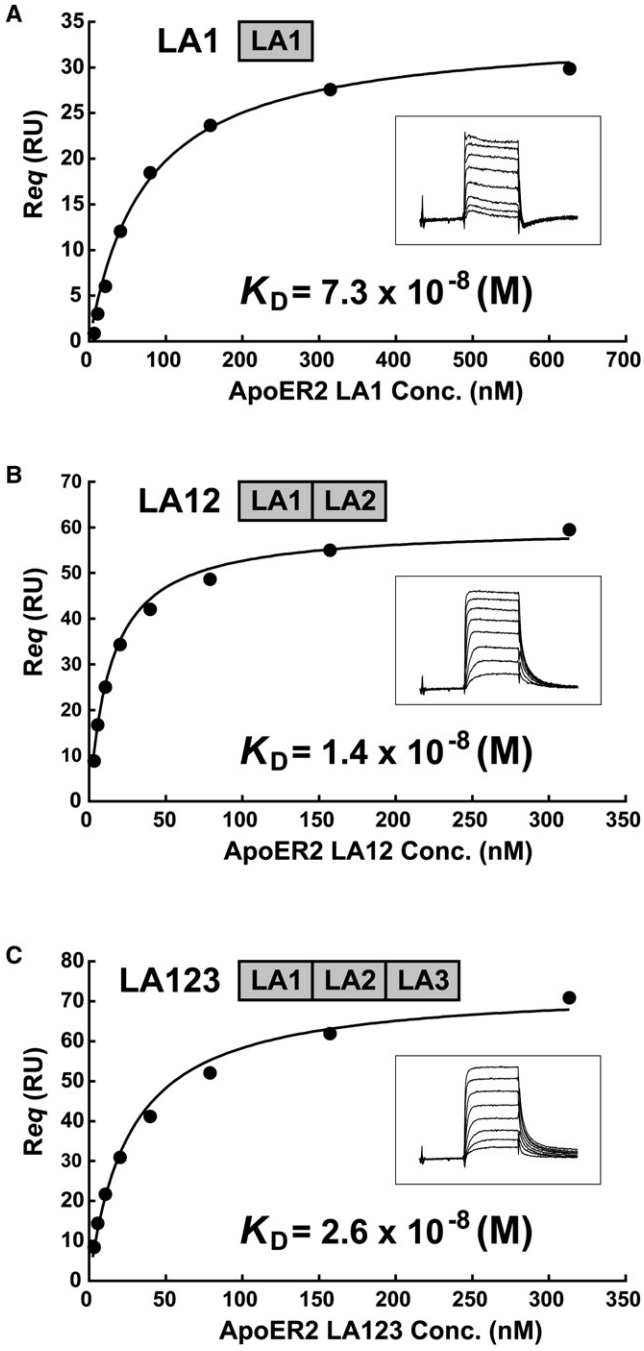

Figure 1. Surface Plasmon Resonance Analysis of the Binding of LA Module Fragments of ApoER2 to Reelin R5-6

Serially diluted LA module fragments (A, LA1; B, LA12; C, LA123) were made to flow over a sensor chip immobilized with reelin R5-6 through Cys2101 to obtain overlaid sensorgrams (inset). Equilibrium response values (generally obtained within 2 min) were plotted against protein concentrations and fitted to the equation described in the Experimental Procedures to calculate the K_D value. The concentration ranges were chosen so that they covered ~0.2 × K_D to 10 × K_D.

of their extracellular domain for reelin binding but also confirms that no other LA modules are required for this interaction. We evaluated the binding affinity of VLDLR LA1 to reelin R5-6 using

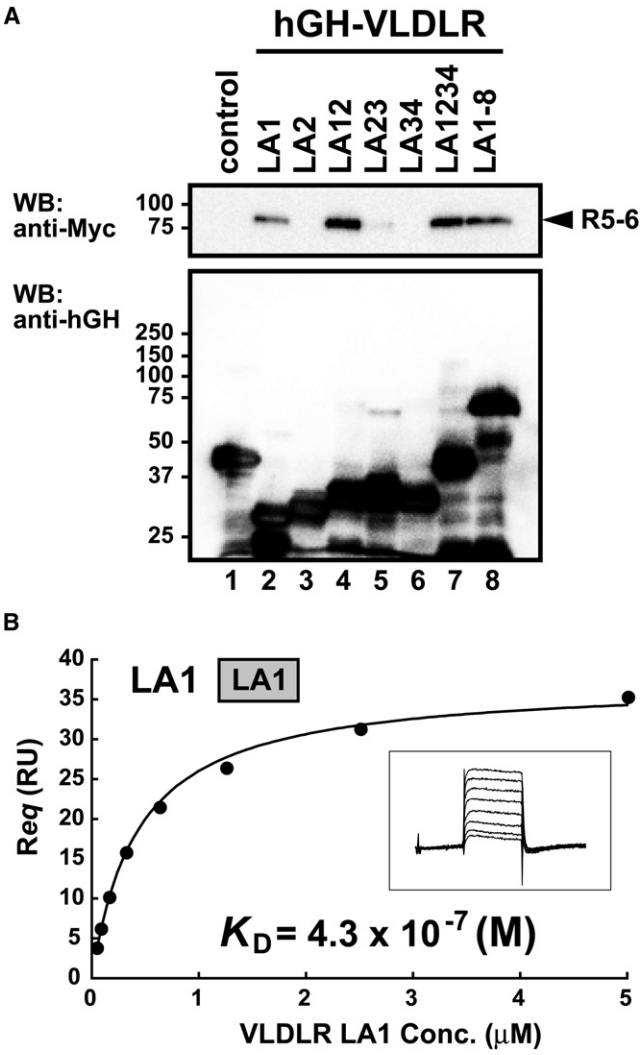

Figure 2. Determination of the Reelin-Binding Unit within VLDLR

(A) hGH fusion proteins containing various numbers of LA modules from VLDLR were captured on anti-hGH antibody-immobilized beads and incubated with culture supernatant containing a reelin R5-6-Myc fragment. Bound R5-6 fragments were detected with anti-Myc antibody (top). The same membrane was reprobed with anti-hGH antisera to confirm that similar amounts of VLDLR fragments were immobilized (bottom). A hGH-ApoER2 LA237 fragment lacking critical LA1 was used as a negative control (lane 1).

(B) SPR analysis of the binding of VLDLR LA1 to reelin R5-6. Because of the lower affinity of VLDLR, the concentration range used was higher than that described in the legend to Figure 1.

SPR (Figure 2B) and isothermal titration calorimetry (Figure S1C) and obtained K_D values of 430 and 880 nM, respectively. Therefore, there is an ~6- to 9-fold difference in the reelin-binding affinity of the core reelin-binding site (i.e., LA1) between ApoER2 and VLDLR. This is consistent with the affinity difference between the two receptor classes reported by Andersen et al. (2003) (see also Discussion section).

The requirement of only a single LA module for stable reelin binding by LDLR family receptors has not been previously reported and is in sharp contrast to other LA module-containing receptors, where at least two consecutive LA modules are

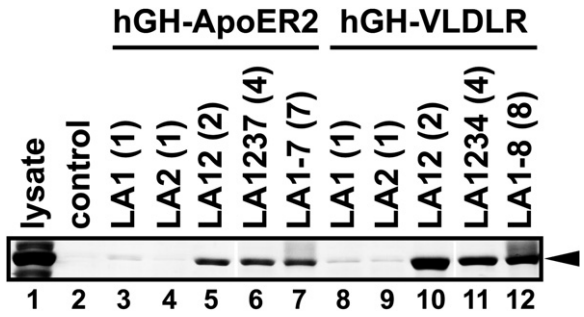

Figure 3. Binding of RAP to LA Module Fragments of Reelin Receptors

Interaction of GST-RAP fusion protein with various LA module fragments of ApoER2 and VLDLR was analyzed by a pull-down binding assay using anti-hGH beads. Each fragment was designated based on the presence of a particular LA module set. The total number of modules contained in the construct is shown in parenthesis. Note that the ApoER2 does not contain LA4–6 because it is the major variant found in the brain (Brandes et al., 2001). The arrowhead indicates the position for the GST-RAP protein.

needed for high-affinity ligand binding (Andersen et al., 2000a, 2000b; Fisher et al., 2004). In order to confirm this difference, we evaluated the ability of various LA module fragments from two reelin receptors to bind the pan-LA module-binding protein, receptor-associated protein (RAP), using the same pull-down assay format. As shown in Figure 3, GST-RAP binding required the presence of at least two LA modules on the receptor side, and no binding was observed for receptor fragments with only one LA module, including LA1. Finally, we checked whether reelin R5-6 and the ApoER2 LA1 fragment form a stable complex in solution by gel filtration. An excess amount of receptor fragment was incubated with the ligand and subjected to gel filtration chromatography in the presence of 2 mM $CaCl_2$. As shown in Figure 4, ~5 kDa LA1 fragment was coeluted with 80 kDa R5-6, suggesting that the ligand-receptor association was strong enough to withstand spontaneous dissociation during the chromatographic run (~30 min). Taken together, reelin is very unique among those protein ligands recognized by the LA module in that it requires only a single module of select receptors.

Overall Structure of the Reelin R5-6/LA1 Complex

In order to unravel the structural basis underlying the unique reelin-receptor interaction, we determined the crystal structure of reelin R5-6 in complex with LA1 from ApoER2, using the R5-6/LA1 complex purified on a gel filtration column described above. Crystals of the complex were obtained in space group $P2_1$ with one reelin:ApoER2 complex in the asymmetric unit. The crystal structure was determined at 2.6 Å resolution by the molecular replacement method using a receptor-unbound form of the reelin R5-6 structure [Protein Data Bank (PDB) code 2E26] as a search model (Figure 5 and Table 1). In the complex, ApoER2 LA1 is bound at the "bottom" of the subrepeat A of R6 near the interface with the R5, but makes no contacts with R5 or subrepeat B of R6 (Figure 5A). The Lys2467 of reelin, determined as the receptor-binding residue by site-directed mutagenesis (Yasui et al., 2007), is indeed located at the interface (discussed later).

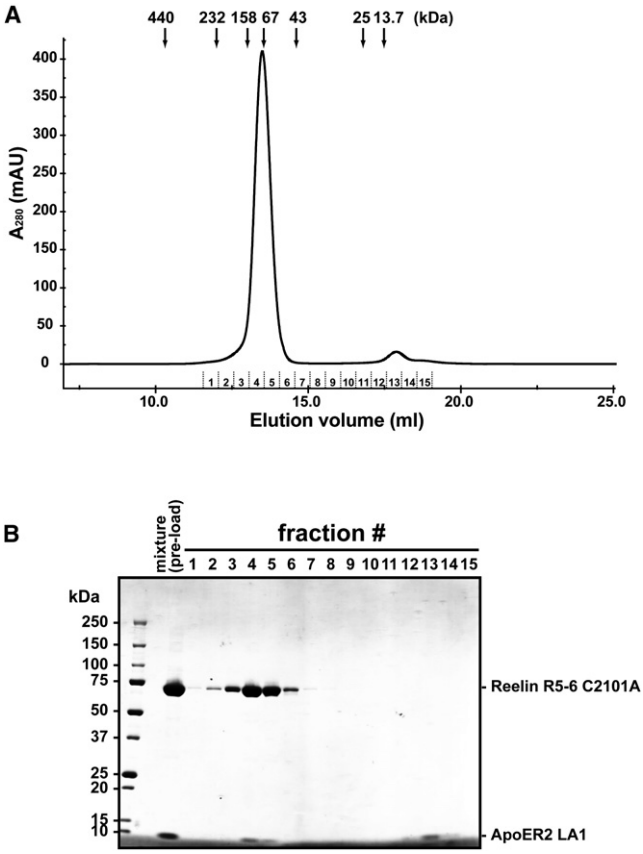

Figure 4. Purification of the Reelin R5-6:ApoER2 LA1 Complex on Gel Filtration Chromatography

(A) Reelin R5-6 C2101A fragment was mixed with an excess molar concentration of ApoER2 LA1 and applied to a Superdex 200 10/300 column equilibrated with 20 mM Tris, 150 mM NaCl, and 2 mM $CaCl_2$ (pH 7.5) at a flow rate of 0.5 ml/min. Positions for molecular weight standard proteins are indicated at the top.

(B) SDS-PAGE analysis of the fractions of a gel filtration chromatography. SDS-PAGE was performed on a 5%–20% gradient gel under non-reducing condition. The proteins were visualized by Coomassie brilliant blue staining.

ApoER2 LA1 in the complex assumed a typical LA module structure with a disulfide-bonding pattern of 1-3, 2-5, 4-6 (Cys47-Cys59, Cys54-Cys72, Cys66-Cys81) and a calcium-binding site. The calcium ion is coordinated by side chains from four conserved acidic residues (Asp67, Asp71, Asp77, and Glu78) and two backbone carbonyl groups (Trp64 and Asp69) in octahedral geometry (Figure 6A). The structure of R5-6 in the complex was essentially identical to that of free R5-6 determined earlier, except for a few loop regions involved in the crystal packing, showing 0.95 Å rmsd for Cα atoms (666 residues) after structural superposition (Figure 5B). This indicates that no major conformational changes occur upon LA1 binding and that R5-6 behaves as a rigid unit during the interaction despite the large size and the modular nature of the fragment. Two zinc ions were previously found on the surface of free R5-6 (Yasui et al., 2007). We have confirmed one of them (bound to the surface of R6) to be present in the current complex. Apparently, the occupancy of the zinc ion is very low, since it shows a very high temperature factor compared with other components of the crystal (Table 1). Nevertheless, an electron density peak was clearly observed in the anomalous difference Fourier map calculated with data taken at zinc absorption peak wavelength (data not shown). This zinc ion, however, was not involved in the contact with LA1 in the crystal structure. Another zinc ion found at a crystal-packing interface involving R5 was not identified in the current complex structure, probably due to the differences in crystal packing.

The Binding Interface: Reelin Side

The total amount of solvent-accessible surface area (ASA) of the interface between R5-6 and LA1 in the complex is 696 Å^2, which is very small when compared to standard-sized physiological protein-protein interfaces (1600 ± 400 Å^2) (Lo Conte et al., 1999). In fact, it is as small as the interfaces between the individual LA module of LDLR and domain 3 of RAP (the interfaces of RAP-LA3 and RAP-LA4 are 731 Å^2 and 696 Å^2, respectively) (Figure 7). As described earlier, RAP-LDLR interaction requires both interfaces (total of 1427 Å^2), highlighting the unusual stability of the reelin-LA1 interaction as mediated by such a small interface. This strong association seems to stem from the presence of several hydrogen bonds and electrostatic interactions across the interface, as well as the van der Waals (vdW) contacts between hydrophobic residues from both sides. Significantly, the reelin interface is particularly rich in hydrophobic residues, compared to either of the RAP D3-LA interfaces (Figure 7). This high proportion of hydrophobic surface area may be the basis for the unusually stable association that exists here despite the use of a very small interface.

From the reelin side, 12 residues are buried upon receptor binding, with the top 6 contributing ~90% of the interface (Table S1). Strikingly, four loops harboring these residues assume main-chain conformation nearly identical to that of free reelin (Figure 5C). This suggests that the entropic cost incurred upon complex formation is relatively low, possibly contributing to the high affinity. We previously reported that reelin Lys2360 and Lys2467 constituted the receptor-binding site and were essential for the induction of Dab1 phosphorylation when tested in the primary culture of neurons (Yasui et al., 2007). The current structure is in complete agreement with this observation. Lys2467 is the most important residue in the interaction (accounting for more than a quarter of the interface), using its ε-amino group to form salt bridges with carboxylates of two calcium ion-coordinating acidic residues (Asp67 and Asp71) and Asp69 in LA1. In addition, its aliphatic portion packs against Trp64, making numerous vdW contacts. This Lys-recognition mode is, in fact, identical to the "canonical" mode of interaction proposed for other LA modules in ligand binding (Blacklow, 2007; Fisher et al., 2006). Lys2360 makes the second largest contribution to the interface (Table S1), mainly through vdW contacts (Figure 6A) and weak electrostatic interaction with Asp 69 of LA1. It is remarkable that about half of the interface is made up of just two Lys residues, with Lys2467 serving as a "core" and Lys2360 as an "auxiliary" residue. A double-Lys/Arg recognition mode, similar to that described above, was noted in RAP-LDLR and hypothesized in apoE4-LDLR (Fisher et al., 2006). In some of the LA module-ligand pair structures, Arg, rather than Lys, functioned as the core basic residue from

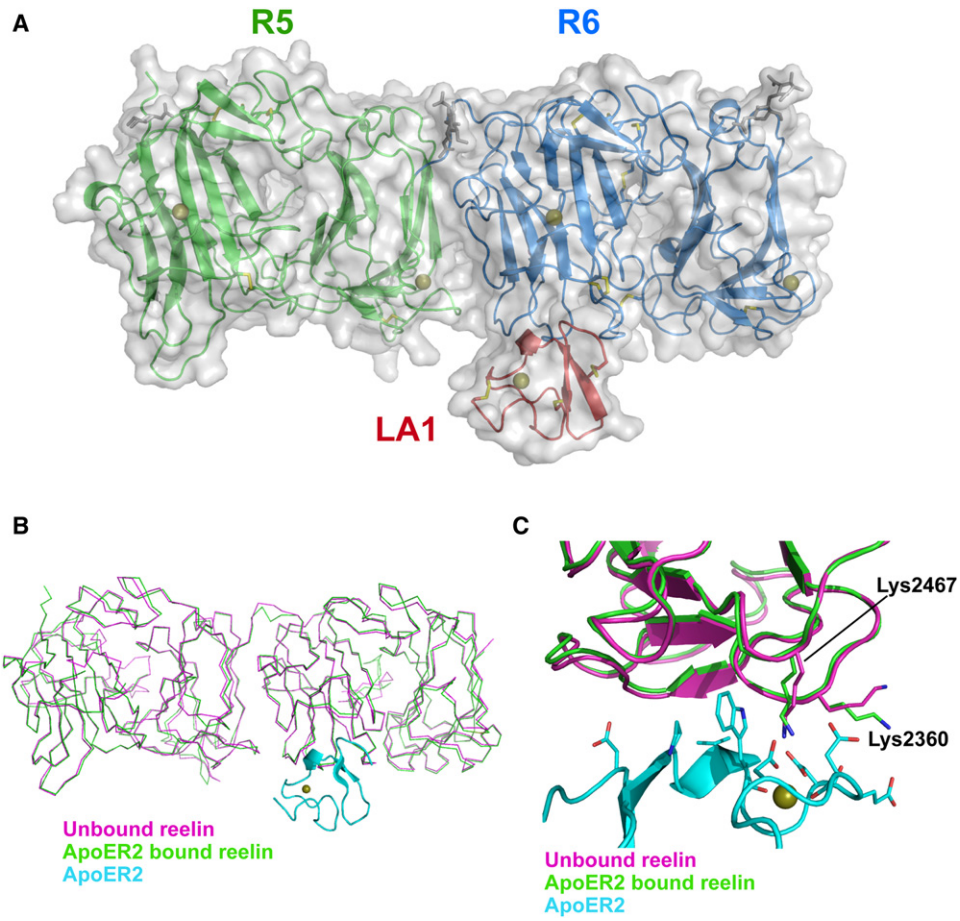

Figure 5. Crystal Structure of the Reelin R5-6:ApoER2 LA1 Complex

(A) Overall structure of the reelin R5-6:ApoER2 LA1 complex. Reelin R5-6 and ApoER2 LA1 polypeptide chains are illustrated by a ribbon model (reelin R5 is colored in green, reelin R6 in blue, and ApoER2 LA1 in red) with a translucent molecular surface. Disulfide bonds (yellow) and *N*-linked sugar chains (gray) are shown as stick models. Ca^{2+} ions are shown as gold spheres. All structure images were prepared using PyMOL (http://www.pymol.org).

(B) Superposition of the reelin R5-6:ApoER2 LA1 complex and the unbound reelin R5-6. The reelin R5-6:ApoER2 LA1 complex is shown with reelin R5-6 in green and ApoER2 LA1 in cyan. The receptor-free reelin R5-6 is shown in magenta.

(C) Close-up view of the region surrounding the binding interface. Lys2360 and Lys2467 are shown as stick models and labeled. Key interacting residues on the LA1 of ApoER2 are also shown as stick models.

the ligands (Blacklow, 2007; Royer et al., 2006). When Lys2467 of reelin was mutated to Arg, however, the mutant R5-6 fragment could no longer bind to full-length ApoER2 (Figure 8A, lane 4). This was probably caused by the clash of longer Arg residue at the interface, since Lys2467 was inserted into the LA1 pocket in a "head-on" fashion. In contrast, the Lys to Arg mutation was tolerated at residue 2360, although the Ala mutation nearly abolished the binding (Figure 8A, lanes 1 and 2). In this case, longer Arg could be accommodated because the side chain was pointing sideways (Figure 6A). Since the Nε atom of Lys2360 was not in a hydrogen-bonding distance from any of the carboxylate oxygens in the complex, the positive charge of the auxiliary residue may be important in long-range electrostatic attractions to the highly electronegative surface of LA1.

The Binding Interface: ApoER2 Side

At the receptor side of the interface, ten residues contribute to the binding (Table S1). Two of them contribute less than 1% and are thus omitted from the following discussion. The most prominent contribution to the ASA was from Trp64, which buried a surprisingly large surface area (109 $Å^2$), which is more than half of the total surface area of a Trp residue (Miller et al., 1987). Apart from the tripartite salt bridge described in the previous section, we noted a hydrogen bond between Nε of Trp64 (LA1) and the backbone carbonyl of Ile2356 (reelin), as well as a water-mediated hydrogen bond network involving Asp67(Oδ1), Val63(O), and Lys2360(N) (Figure 6B). In order to determine the contribution, residue-wise, to reelin recognition, interface residues (i.e., Asp50, Pro61, Val63, Trp64, Glu68, and Asp69) were substituted with Ala or conservative amino acids and tested for binding to R5-6. Asp67 and Asp71 could not be mutated as they were critically involved in calcium coordination, which is necessary for the correct folding of the LA module (Blacklow and Kim, 1996). An Ala substitution of Glu48, which lies far from the binding interface, was also conducted to serve as a control. As expected, the E48A mutant exhibited reelin-binding activity comparable

Table 1. Data Collection and Refinement Statistics

Data Collection and Reduction	
Space group	$P2_1$
Unit cell dimensions	a = 56.98 (Å)
	b = 93.84 (Å)
	c = 73.46 (Å)
	β = 107.4 (°)
Resolution range (Å)	46.9–2.6 (2.74–2.60)
Observed reflections	81,857 (11,311)
Unique reflections	21,990 (3,213)
Completeness (%)	96.5 (99.5)
Redundancy	3.7 (3.5)
R_{merge} (%)	7.4 (37.4)
$<I/\sigma(I)>$	7.5 (1.8)
Refinement	
R_{work} (%)	22.3
R_{free} (%)[a]	29.6
Non-H atoms	5,806
Protein	5,711
Water	19
Oligosaccharide	70
Ca^{2+}	5
Zn^{2+}	1
Rmsd from ideal values	
Bond lengths (Å)	0.009
Bond angles (°)	1.23
Average B factors (Å^2)	
Reelin	
R5A	58.17
R5E	57.13
R5B	58.39
R6A	57.63
R6E	57.38
R6B	57.80
ApoER2	
LA1	56.98
Modifications	
Oligosaccharide	53.67
Ions and Solvents	
Ca^{2+}	54.61
Zn^{2+}	118.94
Water	49.59

[a] R_{free} is the R factor for 5% of the reflections excluded from the refinement.

with that of wild-type LA1 (Figure 8B, lane 1). In contrast, the mutation of Trp64 was not tolerated even with the mildly conservative substitution with His (Figure 8B, lane 5), confirming its central role in the recognition process. An Ala substitution of Val63, which provided the second largest ASA to the interface, yielded a somewhat unexpected result. The binding was significantly reduced but still present (Figure 8B, lane 4), despite the elimination of two methyl groups making direct contact with the reelin residues. In contrast, the mutation of Pro61, which contributed only moderately to the interface, abolished the binding (lane 3), indicating its critical requirement vis-à-vis reelin recognition.

We predicted that the contribution of Asp50 to reelin binding was limited for the following reasons: it is located outside the main interface (comprised of other seven residues); it has no partners for strong electrostatic interaction; and it does not make direct contact with reelin. Despite our prediction, the D50A mutant exhibited decreased reelin-binding activity (Figure 8B, lane 2), similar to the level of the V63A mutant. Conversely, the negative charge of Glu68, which had seemed important due to its relatively close proximity to Lys2360 (Figure 6A), turned out to be dispensable, since the charge-neutralizing E68Q mutant exhibited normal binding to reelin (Figure 8B, lane 6). The mutation of Asp69 to Asn has already been shown to abolish reelin binding in full-length ApoER2 (Andersen et al., 2003). We confirmed this in our own binding assay using LA1 and R5-6 fragments (Figure 8B, lane 7). Furthermore, we found that the Glu substitution of the same residue did not affect binding activity (Figure 8B, lane 8), suggesting that the negative charge at this position was critical for ensuing the activity. The presence of acidic amino acid at the corresponding position had been suggested as a "fingerprint" for the ligand-binding activity of LA modules (Andersen et al., 2003). As the side chain of this residue was sandwiched between the "double Lys" both in our structure (Figure 6B) and in the RAP-LA complex structure, this negative charge may play a key role in stabilizing the ligand-LA complex by bridging these two basic residues.

Comparison between Reelin-Binding and Nonbinding LA Modules

The mutational analyses of ApoER2 LA1 described above indicate that seven out of eight interface residues are required for reelin recognition, with two (Asp67 and Asp71) remaining invariable as Ca^{2+}-coordinating residues, three [Pro61, Trp64, and Asp (or Glu) 69] proving indispensable, and two (Asp50 and Val63) being dispensable but strongly favored to warrant high affinity. We can easily explain why LDLR, which is highly homologous to ApoER2, does not bind reelin since its LA1 lacks the critical acidic residue corresponding to Asp69 (Figure 6C). However, LA1 of VLDLR, the only module that has a reelin-binding capacity other than ApoER2 LA1, shows some disparity from the above pattern (Asp50 → Ser, Pro61 → Thr, Val63 → Leu). Furthermore, a sequence alignment of different LA modules readily identifies several LA modules that partially fulfill the requirement (Figure 6C), yet exhibit no reelin-binding capacity of their own. When one such LA module (LA4 of LDLR) was engineered to emulate the "complete reelin interface" by grafting the interface residues found in ApoER2, it failed to exhibit any reeling-binding activity (Figure S2). We have therefore concluded that reelin-binding specificity cannot be conferred simply by emulating the interface of the final complex.

DISCUSSION

The LDL receptor protein family, which now includes nine members, binds many ligands including protease-protease

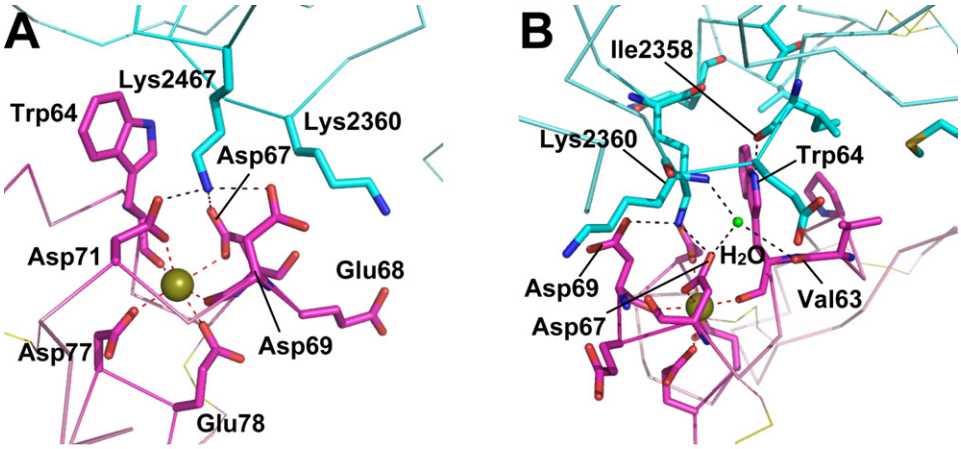

C

```
                          *              * **   *** *
ApoER2_LA1    45 ----KECE-KDQFQCRNE--RCIPSVWRCDEDDDCLDHSDE--DDCPK------ 83
ApoER2_LA2    84 ----KTCA-DSDFTCDNG--HCIHERWKCDGEEECPDGSDESEATCTK------ 134
ApoER2_LA3   135 ----QVCP-AEKLSCGPTSHKCVPASWRCDGEKDCEGGADEA--GCAT------ 175
ApoER2_LA7   312 ----GTCR-GDEFQCGDG--TCVLAIKHCNQEQDCPDGSDE--AGCLQGL---- 352

VLDLR_LA1     28 -GRKAKCE-PSQFQCTNG--RCITLLWKCDGDEDCVDGSDE--KNCVK------ 69
VLDLR_LA2     70 ----KTCA-ESDFVCNNG--QCVPSRWKCDGDPDCEDGSDESPEQCHM------ 110
VLDLR_LA3    111 ----RTCR-IHEISCGAHSTQCIPVSWRCDGENDCDSGEDEE--NCGN------ 151
VLDLR_LA4    152 ----ITCS-PDEFTCSSG--RCISRNFVCNGQDDCSDGSDE--LDCAP------ 190
VLDLR_LA5    191 ----PTCG-AHEFQCSTS--SCIPISWVCDDDADCSDQSDESLEQCGRQ-PV-- 234
VLDLR_LA6    235 --IHTKCP-ASEIQCGSG--ECIHKKWRCDGDPDCKDGSDE--VNCPS------ 275
VLDLR_LA7    276 ----RTCR-PDQFECEDG--SCIHGSRQCNGIRDCVDGSDE--VNCKN------ 314
VLDLR_LA8    315 ---VNQCLGPGKFKCRSG--ECIDISKVCNQEQDCRDWSDEPLKECHI------ 358

LDLR_LA1      23 --VGDRCE-RNEFQCQDG--KCISYKWVCDGSAECQDGSDESQETC-------- 63
LDLR_LA2      64 --LSVTCK-SGDFSCGGRVNRCIPQFWRCDGQVDCDNGSD----GC-------- 103
LDLR_LA3     104 --PPKTCS-QDEFRCHDG--KCISRQFVCDSDRDCLDGSDE--ASC-------- 142
LDLR_LA4     143 --PVLTCG-PASFQCN--SSTCIPQLWACDNDPDCEDGSDEWPQRCRGLYVFQG 191
LDLR_LA5     192 --DSSPCS-AFEFHCLSG--ECIHSSWRCG--PDCKDKSDE--ENC-------- 228
LDLR_LA6     229 --AVATCR-PDEFQCSDG--NCIHGSRQCDREYDCKDMSDE--VGC-------- 267
LDLR_LA7     268 -VNVTLCEGPNKFKCHSG--ECITLDKVCNMARDCRDWSDEPIKEC-------- 310
```

Figure 6. The Reelin-ApoER2 Interface

(A and B) Two different views of the reelin-receptor interface. Reelin R5-6 and ApoER2 LA1 are shown in cyan and magenta, respectively, and Ca^{2+} ion bound to ApoER2 LA1 as a gold sphere. Key interacting residues are shown as stick models and labeled. Hydrogen bonds and the Ca^{2+} coordination are indicated by black and red dashed lines, respectively. Water molecule is shown as green sphere.

(C) Sequence alignment of LA modules from human ApoER2, human VLDLR, and human LDLR. Acidic residues, basic residues, and conserved six Cys residues that formed disulfide bonds are highlighted in red, blue, and gray, respectively. Positions for the eight interface residues in ApoER2 LA1 described in the text are denoted by asterisks above the alignment. LA4 through LA6 of ApoER2 are missing in the major variant expressed in the brain and were thus excluded from the alignment (Brandes et al., 2001).

inhibitor complexes, viruses, signaling molecules, and lipoprotein particles (Nykjaer and Willnow, 2002; Strickland et al., 2002; Willnow et al., 2007). Most of the ligands associated with the LDLR family proteins are recognized by a small structural unit called the LA module that appears as a cluster within the receptor ectodomain. Previous studies have suggested that LA modules generally have the potential to recognize a Lys residue by using a set of conserved residues (Fisher et al., 2006;

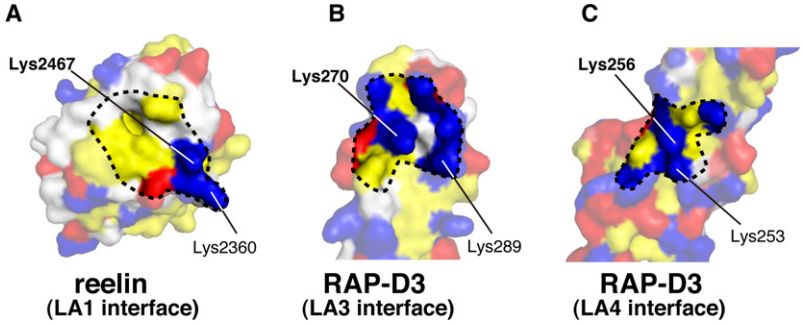

Figure 7. Surface Chemical Properties of LA Module Ligands

Molecular surfaces for reelin R6 (A) and RAP-D3 (B and C) are shaded according to the residue type (red, acidic; blue, basic; yellow, hydrophobic; white, neutral). Interface areas buried upon receptor binding are indicated by broken lines. Primary and auxiliary Lys residues in each interface are labeled by bold and regular type, respectively.

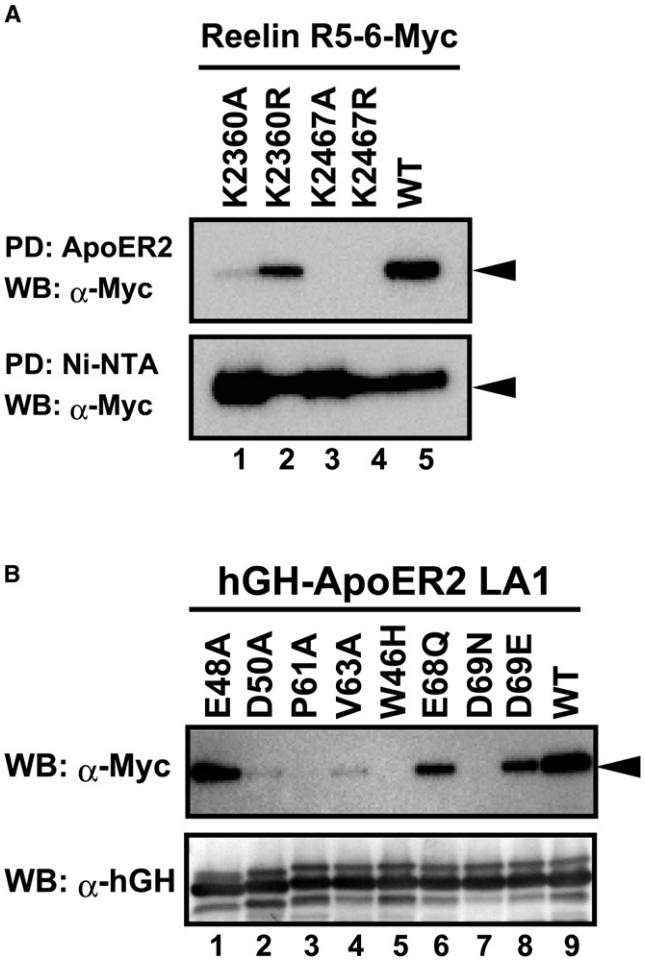

Figure 8. Mutational Analyses of the Interaction between Reelin and ApoER2

(A) The binding of R5-6 mutants with C-terminal Myc+His tag to full-length ApoER2/hGH fusion protein was analyzed with a solid-phase binding assay followed by western blotting using an anti-Myc antibody (top). The same culture supernatants containing R5-6/Myc-His were precipitated with Ni-NTA agarose to compare the expression level among the mutants (bottom). The arrowheads indicate the position for reelin R5-6 protein.

(B) The binding of the R5-6/MycHis fragment to various hGH-ApoER2 LA1 mutants was analyzed by a solid-phase binding assay. Bound reelin R5-6-Myc fragments were detected by western blotting using an anti-Myc antibody (top). The same membrane was reprobed with anti-hGH antisera to compare the expression level of hGH-ApoER2 LA1 mutants (bottom).

Rudenko et al., 2002; Verdaguer et al., 2004). This is in perfect accordance with the promiscuous nature of LA module-containing receptors and explains why multiple LA modules need to be present, since such recognition would not bear meaningful specificity and affinity unless presented in multiple fashion to achieve avidity. Among ~40 residues that make up an LA module, 10 are invariant because they are involved in Ca^{2+} coordination and disulfide bonds, while many other positions are also highly conserved due to the structural requirements of a small domain (Figure 6C), making variations in this module very limited. In other words, the LA module is not an ideal structural scaffold to create a highly specific binding domain.

For those receptors whose primary function is to bind a group of substances for cellular uptake, such promiscuous ligand-binding specificity is not only acceptable but even desirable. For signaling receptors, however, the ability to recognize ligands in a very strict fashion is critical in order to ensure that cells receive signals at the right timing and at the right place. Therefore, reelin receptors must have acquired additional features to ensure this specific recognition of their biological ligand, for example, by increasing the size of the interaction interface. Yet contrary to such an expectation, the data presented here reveals that reelin receptors use unusually small surface areas for recognition. Through mutational analysis we confirmed that most residues at the interface are indeed critically involved in the binding process. However, reelin recognition specificity could not be translated into a simple consensus amino acid motif. Indeed, even the complete "grafting" of the reelin-binding interface onto a non-binding LA module failed to confer any reelin-binding ability (Figure S2B, lane 2). It is likely that non-interface residues of LA1 contribute to the binding event, which underscores the difficulties involved in predicting the physiological protein-protein binding interface even from a three-dimensional structure, particularly when these interactions use small interface areas.

Previous mutational analyses have demonstrated that Lys2360 and Lys2467 within the sixth reelin repeat are critical for receptor binding and cellular signaling (Yasui et al., 2007). Analysis of the crystal structure revealed that they indeed constitute a major part of the binding interface and that Asp69 of ApoER2 plays a critical role in bridging the two Lys residues through its negatively charged side chain (Figure 6A). It is noteworthy that Asp69 within ApoER2 LA1 corresponds to the fingerprint acidic residue described by Andersen et al. (2000a, 2000b, 2001a, 2001b, 2003) as being critical for ligand binding. This double-Lys recognition mode has also been found in other ligand-LA module complexes. In the complex between LDLR and RAP-D3, Lys253 and Lys256 of RAP-D3 are recognized by LA4, while Lys270 and Lys289 are recognized by LA3 (Fisher et al., 2006) (Figure 7). It was also pointed out by Fisher et al. (2006) that Lys143 and Lys 146 of the ApoE4 receptor-binding domain may be involved in the recognition carried out by LA modules of LDLR (Fisher et al., 2006). Two Lys residues in a receptor-binding domain of α_2-macroglobulin have also been implicated in the binding to LA modules of LRP (Nielsen et al., 1996). These observations strongly suggest that the recognition of a primary residue and an auxiliary Lys residue, via an aromatic residue and a bridging fingerprint acidic residue, is the general mode of binding shared among members of the LDLR protein family. In general, Lys-mediated binding is not expected to bear high-affinity outcomes since immobilization of a highly flexible Lys side chain entails a high entropy cost (Derewenda and Vekilov, 2006). Consequently, the ligand-binding ability of a single LA module is generally low, as exemplified by the LA-RAP interaction (Figure 3). In contrast, reelin-LA1 complex has reasonably high affinity. This uniquely strong interaction can be reconciled by the predominantly hydrophobic nature of the reelin-LA1 interface, in contrast to the mainly hydrophilic/electrostatic nature of RAP-LA interfaces (Figure 7). Another unique feature of the reelin-LA1 interface is the peripheral location of the primary Lys residue, in sharp contrast to

the RAP-LA interfaces where the primary Lys occupies the "bull's-eye" position (Figure 7). This peripheral location may minimize the high immobilization entropy cost of the Lys upon the onset of complex formation.

We show that there is an ~6- to 9-fold difference in the binding affinity between ApoER2 LA1 and VLDLR LA1 (Figures 1A and 2B; Figures S1A and S1C). This difference is consistent with what Andersen et al. (2003) have reported using full-length receptor ectodomain fragments (0.2 nM for ApoER2 and 1.2 nM for VLDLR), except that the affinity values were ~400-fold lower. This discrepancy can at least partly be explained by the fact that Andersen et al. (2003) used partially purified full-length reelin protein that exists as multimers, in sharp contrast to the monomeric R5-6 fragment used in this study. It is also possible that domains other than the R5-6 segment of reelin [such as R3-4, which is also present in the R3–6 fragment found in tissues (Jossin et al., 2007)] have some weak affinity for ApoER2, thereby enhancing the overall affinity. Another important possibility is that EGF modules and/or the YWTD β-propeller domains of reelin receptors may have a weak affinity for reelin. Interestingly, we found that the dissociation rate of full-length ApoER2 ectodomain (ApoER2 ECΔ4–6) from the monomeric R5-6 fragment was slower than the LA123 (Figure S3), even though none of the domains outside LA1 possessed detectable binding affinity (Yasui et al., 2007). We have concluded that the LA1 module is used by both receptors as the primary reelin-docking machinery, although the observed subnanomolar physiological affinity may stem from the multimeric nature of reelin and the indirect contribution of auxiliary modules outside LA1/R5-6.

Another unique feature of reelin/LA1 interaction is the lack of His residues near the interface. As RAP functions as an escort protein for LA module-containing receptors during the biosynthesis (Bu et al., 1995), it must be dissociated to allow maturation and the correct transport of the receptors. It has been postulated that the presence of multiple partially buried His residues in the RAP-D3 act as the pH sensor and facilitate dissociation of the RAP-receptor complex at the Golgi's acidic pH (i.e., <6.5) by destabilizing the D3 (Lee et al., 2006). In reelin R6, the closest His residue is more than 15 Å away from the interface and completely solvent exposed, making it difficult to affect the association/dissociation kinetics either directly or indirectly. In fact, interaction between reelin R5-6 and ApoER2 was unchanged at pH 7.5 and 6.0 (data not shown).

It is noteworthy that both ApoER2 and VLDLR recognize reelin using their extreme N-terminal LA module. Reelin is a gigantic glycoprotein with 3461 amino acids and is known to exist as disulfide-linked oligomers in the brain (Kubo et al., 2002; Utsunomiya-Tate et al., 2000). Recognition of such a bulky ligand using the extracellular "tip" of the receptors seems appropriate considering the steric impedance involved. In addition, the location of a reelin-binding site at this N terminus may also affect the intracellular fate of the reelin/receptor complex for the following reason. Examination of the crystal structure of the full-length LDLR ectodomain at pH 5.3 revealed intramolecular docking of the LA4-5 segment, mediated by protonated His residues, onto the β-propeller domain (Rudenko et al., 2002), leading to the hypothesis that the internal ligand (i.e., β-propeller) replaces the bound ligand, facilitating ligand release at an endosomal pH (Beglova et al., 2004). This same pH-dependent internal docking mechanism is likely to operate in the reelin receptors ApoER2 and VLDLR since they share the same domain arrangement with LDLR. In this scenario, however, the N-terminal LA module (i.e., LA1) would not compete with the β-propeller domain, resulting in sustained reelin binding at a moderately acidic endosomal pH. Together with the absence of the His-switch mechanism described above, this may lead to the more distant transport of reelin along the endocytic pathway compared to the typical lipoprotein ligands following cellular internalization. It is tempting to speculate that the intracellular events involving reelin that occur long after the ligand binding and internalization may constitute the important part of the reelin-signaling pathway that ultimately changes the migration behavior of the neurons.

EXPERIMENTAL PROCEDURES

Construction of Expression Vectors

The expression construct for the reelin R5-6 fragment containing the signal sequence of mouse nidogen-1 at the N terminus, as well as a tobacco etch virus (TEV) protease cleavage site, followed by a Myc tag and octahistidines at the C terminus, was carried out as previously described (Nogi et al., 2006). Cys2101 was mutated to Ala using QuickChange strategy (Stratagene). LA module segments of VLDLR and LDLR were amplified from the respective cDNAs (gifts from T. Yamamoto, Tohoku University) (Sakai et al., 1994; Yamamoto et al., 1984) and fused to the C terminus of hGH minigene using a pSGHV0 vector (Leahy et al., 2000). The residue numbers for each of the VLDLR fragments were as follows: LA1–8, 28–358; LA1234, 28–190; LA12. 28–110; LA1, 28–69; LA2, 70–110 (amino acid numbering is from the precursor polypeptide sequence). The LDLR LA4 fragment encoded Pro143-Cys182. hGH fusion constructs containing various length of ApoER2 (e.g., hGH-ApoER2 LA1) were generated as described previously (Yasui et al., 2007). The amino acid substitution mutations were introduced into the expression vectors by using QuickChange strategy (Stratagene). To construct expression plasmids for the glutathione-S-transferase (GST)-fused LA module fragments (pGEX-HT-ApoER2 LA1, pGEX-HT-ApoER2 LA12, pGEX-HT-ApoER2 LA123, and pGEX-HT-VLDLR LA1), DNA fragments corresponding to the reelin receptors were cloned into pGEX-HT, a modified version of pGEX-3T (GE Healthcare) that contains an octahistidine and a TEV protease cleavage site upstream of the cloning site. For GST-RAP, a DNA fragment spanning amino acid residue Tyr35-Leu357 of the mouse RAP sequence flanked by BamHI and EcoRI was amplified by PCR from mouse RAP cDNA (a gift from G. Bu, Washington University School of Medicine) (Bu et al., 1995) using the following primer set: 5′-CGGGATCCTACTCGCGGGAGAAG AAC-3′ (forward) and 5′-CGGAATTCTCAGAGTTCGTTGTGCCG-3′ (reverse). The amplified DNA fragment was cloned into the BamHI-EcoRI site of pGEX-HT. All constructs were verified by DNA sequencing.

Protein Expression and Purification

For stable expression of reelin R5-6 C2101A, Chinese hamster ovary lec.3.2.8.1 cells (Stanley, 1989) were transfected with expression plasmid as described previously (Nogi et al., 2006). Briefly, transfected cells were plated in 96-well plates and selected for resistance against 1.5 mg/ml G418 (Nakalai Tesuque). The clone with the highest secreted levels of the reelin R5-6 C2101A fragment was cultured in roller bottle (CORNING). The reelin R5-6 C2101A fragment was purified from culture supernatants by ammonium sulfate precipitation and Ni-NTA agarose chromatography. Further purification was carried out by gel filtration chromatography and anion-exchange chromatography on MonoQ 5/50GL (GE Healthcare).

LA module fragments of ApoER2 (LA1, LA12, and LA123) and VLDLR (LA1) were expressed as GST fusion proteins in *E. coli* BL21 (DE3). Protein expression was induced by the addition of 0.5 mM isopropyl-β-*D*-thiogalactopyranoside. Cells were cultured for 4 hr at 37°C, harvested by centrifugation, resuspended in 10 mM Tris (pH 8.0), 300 mM NaCl, and 10 mM imidazole, and lysed

by sonication. After removing the cell debris by centrifugation, the supernatant containing the fusion proteins were collected and then applied on a Ni-NTA agarose column (QIAGEN). After washing the column with 20 mM imidazole, 300 mM NaCl, and 20 mM Tris (pH 8.0), proteins were eluted with 250 mM imidazole, 300 mM NaCl, and 20 mM Tris (pH 8.0). The fusion proteins were treated with His-tagged TEV protease to release the GST plus the octahistidine tag. TEV protease and GST-octahistidine were then removed by the second Ni-NTA agarose chromatography and flow through fraction was collected. LA module fragments were refolded by dialysis at 4°C against 50 mM Tris (pH 8.0), 10 mM $CaCl_2$, 2 mM L-cysteine, and 0.5 mM L-cystine according to the protocol described by Fisher et al. (2004). Refolded LA module fragments were further purified on a MonoQ 5/50GL anion-exchange column. The column was equilibrated with 20 mM Tris (pH 8.0) and 2 mM $CaCl_2$ and elution was performed by a linear gradient from 0 to 1 M NaCl over a 20-column volume at a flow rate of 2 ml/min. The fractions containing refolded proteins were pooled and concentrated using an ultrafiltration. Refolded LA module fragments were analyzed by SDS-PAGE under non-reducing and reducing conditions as a validation of native folding and disulfide bond formation (Bajari et al., 2005). Protein concentration of LA modules were determined using extinction coefficients (ε_{280}, $M^{-1}cm^{-1}$) estimated according to the method of Gill and von Hippel (1989).

To purify the reelin R5-6 C2101A in a complex with ApoER2 LA1, R5-6 fragments were mixed with LA1 (5-fold molar excess) and applied to gel filtration chromatography using a Superdex200 10/300 GL column. The fractions containing reelin R5-6 and ApoER2 LA1 were pooled and then concentrated to 11 mg/ml in a buffer containing 150 mM NaCl, 2 mM $CaCl_2$, and 20 mM Tris (pH 7.5) using Ultrafree (MWCO 3,000) (Millipore).

Crystallization, Data Collection, and Structural Determination

Initial crystallization conditions were found by screening using the Precipitant Synergy67 Kit (Emerald BioSystems) (Majeed et al., 2003) and the hanging drop vapor-diffusion method. Crystals with different morphologies appeared under various conditions. Finally, diffraction-quality plate-like crystals were obtained through vapor diffusion at 20°C in hanging drops containing equal volume of protein and the well solution containing 21%–25% PEG1000, 12.5%–15% 2 MPD, and 100 mM HEPES (pH 7.5) after 5 days.

Before data collection, crystals were cryoprotected with 36%–38% MPD, 21%–25% PEG1000, and 100 mM HEPES (pH 7.5) and flash-frozen in liquid nitrogen. Diffraction data were collected at beamline BL44-XU of SPring-8. Data sets were processed with HKL2000 (Otwinowski and Minor, 1997). The structure of the reelin R5-6:ApoER2 LA1 complex was determined at 2.6 Å by the molecular replacement method using the atomic coordinates of reelin R5-6 (PDB code 2E26) as a search model. The program MOLREP (Vagin and Teplyakov, 1997) located one R5-6 molecule in the asymmetric unit. The ApoER2 LA1 model was manually built against a weighted F_o–F_c electron density map following molecular replacement. Manual model fitting was performed using Coot (Emsley and Cowtan, 2004), followed by refinement with REFMAC5 (Murshudov et al., 1997). In the final stage of model building, translation/libration/screw parameters were included in the refinement. Several rounds of model fitting and refinement resulted in an R factor of 22.3% and a free R factor of 29.6%. The quality of the final model was validated using MolProbity (Lovell et al., 2003). 93.80% of the residues were in the favored regions of the Ramachandran plot, while 0.56% (Asn-2272, Gly-2320, Ala-2385, and Pro-2417) were assigned as outliers. Data collection and refinement statistics are summarized in Table 1. The binding of the zinc ion on the R6 surface was confirmed by calculating the anomalous difference Fourier map with the diffraction data set collected near the absorption edge of zinc. Data collection for zinc identification was performed at Photon Factory BL-17A.

Solid-Phase Binding Assay

A solid-phase binding assay to evaluate the binding of reelin to the hGH fusion proteins of its receptors was carried out as previously described (Nogi et al., 2006). To analyze the RAP-receptor interactions, *E. coli* lysate containing the GST-RAP fusion protein (100 μl) was mixed with 400 μl of TBS and incubated with 10 μl of receptor-captured beads, followed by incubation at 4°C for 1 hr. After washing, proteins retained on the beads were eluted by adding 2× SDS-PAGE sample buffer, separated by SDS-PAGE, and then stained with Coomassie brilliant blue.

Surface Plasmon Resonance Analysis

SPR analysis was carried out with a Biacore2000 instrument (GE Healthcare) as previously described with slight modifications (Yasui et al., 2007). Wild-type reelin R5-6 fragment, which retained intact Cys2101, was biotinylated with PEO-Maleimide-activated biotin (Thermo Scientific) as previously described (Yasui et al., 2007). Biotinylated R5-6 was allowed to flow onto a streptavidin-coated sensor chip at a concentration of 30 μg/ml, resulting in the immobilization of ~1500 RU of ligand. Sensorgrams were collected after infusing various concentrations of LA module fragments analyte in 20 mM Tris (pH 7.5), 150 mM NaCl, 2 mM $CaCl_2$, and 0.005% Tween20 at a flow rate of 10 μl/min. The surface was regenerated by a pulse infusion of 20 mM Tris (pH 7.5), 20 mM EDTA, and 1 M NaCl after each run, which did not deteriorate the binding capacity of the immobilized ligand. Values for the apparent dissociation constants (K_D) were calculated from equilibrium binding data at six protein concentrations differing by 2-fold in the range of 4.88 nM to 625 nM for ApoER2 LA1, 2.44 nM to 312.5 nM for ApoER2 LA12 and LA123, and 39 nM to 5 μM for VLDLR LA1, respectively. Data were directly fitted using the following equation by least square method: $R_{eq} = K_A \times C \times R_{max}/(1 + K_A \times C)$, where R_{eq} is the response at equilibrium corrected for bulk refractive index errors using a mock-coupled flow cell blocked with ethanolamine, C is the analyte (i.e., LA module fragment) concentration, and K_A is the association constant.

ACCESSION NUMBERS

The atomic coordinates of the reelin R5-6:ApoER2 LA1 complex were deposited in the protein data bank under accession number 3A7Q.

SUPPLEMENTAL INFORMATION

Supplemental Information includes three figures and one table and can be found with this article online at doi:10.1016/j.str.2010.01.010.

ACKNOWLEDGMENTS

We would like to thank Y. Yamada, N. Matsugaki, and N. Igarashi of Photon Factory and E. Yamashita, M. Yoshimura, M. Suzuki, and A. Nakagawa of SPring-8 BL-44XU for their help with X-ray data collection; K. Tamura-Kawakami, E. Mihara, and M. Nampo for their excellent technical support; S. Tabata for preparation of LA module proteins; and M. Nakano for preparation of the manuscript. This work was partly supported by the Grant-in-Aid for Scientific Research (A) from the Ministry of Education, Culture, Sports, Science and Technology of Japan (MEXT), by the Grant-in-Aid for Scientific Research on Priority Areas from MEXT, and by the Protein 3000 Project grant from MEXT. The authors declare that they have no competing financial interests.

Received: October 7, 2009
Revised: January 12, 2010
Accepted: January 20, 2010
Published: March 9, 2010

REFERENCES

Andersen, O.M., Christensen, L.L., Christensen, P.A., Sorensen, E.S., Jacobsen, C., Moestrup, S.K., Etzerodt, M., and Thogersen, H.C. (2000a). Identification of the minimal functional unit in the low density lipoprotein receptor-related protein for binding the receptor-associated protein (RAP). A conserved acidic residue in the complement-type repeats is important for recognition of RAP. J. Biol. Chem. *275*, 21017–21024.

Andersen, O.M., Christensen, P.A., Christensen, L.L., Jacobsen, C., Moestrup, S.K., Etzerodt, M., and Thogersen, H.C. (2000b). Specific binding of alpha-macroglobulin to complement-type repeat CR4 of the low-density lipoprotein receptor-related protein. Biochemistry *39*, 10627–10633.

Andersen, O.M., Petersen, H.H., Jacobsen, C., Moestrup, S.K., Etzerodt, M., Andreasen, P.A., and Thogersen, H.C. (2001a). Analysis of a two-domain binding site for the urokinase-type plasminogen activator-plasminogen

activator inhibitor-1 complex in low-density-lipoprotein-receptor-related protein. Biochem. J. *357*, 289–296.

Andersen, O.M., Schwarz, F.P., Eisenstein, E., Jacobsen, C., Moestrup, S.K., Etzerodt, M., and Thogersen, H.C. (2001b). Dominant thermodynamic role of the third independent receptor binding site in the receptor-associated protein RAP. Biochemistry *40*, 15408–15417.

Andersen, O.M., Benhayon, D., Curran, T., and Willnow, T.E. (2003). Differential binding of ligands to the apolipoprotein E receptor 2. Biochemistry *42*, 9355–9364.

Bajari, T.M., Strasser, V., Nimpf, J., and Schneider, W.J. (2005). LDL receptor family: isolation, production, and ligand binding analysis. Methods *36*, 109–116.

Beglova, N., Jeon, H., Fisher, C., and Blacklow, S.C. (2004). Cooperation between fixed and low pH-inducible interfaces controls lipoprotein release by the LDL receptor. Mol. Cell *16*, 281–292.

Blacklow, S.C. (2007). Versatility in ligand recognition by LDL receptor family proteins: advances and frontiers. Curr. Opin. Struct. Biol. *17*, 419–426.

Blacklow, S.C., and Kim, P.S. (1996). Protein folding and calcium binding defects arising from familial hypercholesterolemia mutations of the LDL receptor. Nat. Struct. Biol. *3*, 758–762.

Brandes, C., Kahr, L., Stockinger, W., Hiesberger, T., Schneider, W.J., and Nimpf, J. (2001). Alternative splicing in the ligand binding domain of mouse ApoE receptor-2 produces receptor variants binding reelin but not alpha 2-macroglobulin. J. Biol. Chem. *276*, 22160–22169.

Bu, G., Geuze, H.J., Strous, G.J., and Schwartz, A.L. (1995). 39 kDa receptor-associated protein is an ER resident protein and molecular chaperone for LDL receptor-related protein. EMBO J. *14*, 2269–2280.

D'Arcangelo, G., Miao, G.G., Cheng, S.C., Soares, H.D., Morgen, J.I., and Curran, T. (1995). A protein related to extracellular matrix proteins mutant reeler. Nature *374*, 719–723.

Derewenda, Z.S., and Vekilov, P.G. (2006). Entropy and surface engineering in protein crystallization. Acta Crystallogr. D Biol. Crystallogr. *62*, 116–124.

Emsley, P., and Cowtan, K. (2004). Coot: model-building tools for molecular graphics. Acta Crystallogr. D Biol. Crystallogr. *60*, 2126–2132.

Fisher, C., Abdul-Aziz, D., and Blacklow, S.C. (2004). A two-module region of the low-density lipoprotein receptor sufficient for formation of complexes with apolipoprotein E ligands. Biochemistry *43*, 1037–1044.

Fisher, C., Beglova, N., and Blacklow, S.C. (2006). Structure of an LDLR-RAP complex reveals a general mode for ligand recognition by lipoprotein receptors. Mol. Cell *22*, 277–283.

Gill, S.C., and von Hippel, P.H. (1989). Calculation of protein extinction coefficients from amino acid sequence data. Anal. Biochem. *182*, 319–326.

Herz, J., and Bock, H.H. (2002). Lipoprotein receptors in the nervous system. Annu. Rev. Biochem. *71*, 405–434.

Howell, B.W., Hawkes, R., Soriano, P., and Cooper, J.A. (1997). Neuronal position in the developing brain is regulated by mouse disabled-1. Nature *389*, 733–737.

Ichihara, H., Jingami, H., and Toh, H. (2001). Three novel repetitive units of reelin. Brain Res. Mol. Brain Res. *97*, 190–193.

Jossin, Y., Bar, I., Ignatova, N., Tissir, F., De Rouvroit, C.L., and Goffinet, A.M. (2003). The reelin signaling pathway: some recent developments. Cereb. Cortex *13*, 627–633.

Jossin, Y., Ignatova, N., Hiesberger, T., Herz, J., Lambert de Rouvroit, C., and Goffinet, A.M. (2004). The central fragment of Reelin, generated by proteolytic processing in vivo, is critical to its function during cortical plate development. J. Neurosci. *24*, 514–521.

Jossin, Y., Gui, L., and Goffinet, A.M. (2007). Processing of Reelin by embryonic neurons is important for function in tissue but not in dissociated cultured neurons. J. Neurosci. *27*, 4243–4252.

Kim, D.H., Iijima, H., Goto, K., Sakai, J., Ishii, H., Kim, H.J., Suzuki, H., Kondo, H., Saeki, S., and Yamamoto, T. (1996). Human apolipoprotein E receptor 2. A novel lipoprotein receptor of the low density lipoprotein receptor family predominantly expressed in brain. J. Biol. Chem. *271*, 8373–8380.

Koch, S., Strasser, V., Hauser, C., Fasching, D., Brandes, C., Bajari, T.M., Schneider, W.J., and Nimpf, J. (2002). A secreted soluble form of ApoE receptor 2 acts as a dominant-negative receptor and inhibits Reelin signaling. EMBO J. *21*, 5996–6004.

Kohno, S., Kohno, T., Nakano, Y., Suzuki, K., Ishii, M., Tagami, H., Baba, A., and Hattori, M. (2009). Mechanism and significance of specific proteolytic cleavage of Reelin. Biochem. Biophys. Res. Commun. *380*, 93–97.

Kubo, K., Mikoshiba, K., and Nakajima, K. (2002). Secreted Reelin molecules form homodimers. Neurosci. Res. *43*, 381–388.

Kuo, G., Arnaud, L., Kronstad-O'Brien, P., and Cooper, J.A. (2005). Absence of Fyn and Src causes a reeler-like phenotype. J. Neurosci. *25*, 8578–8586.

Lambert de Rouvroit, C., de Bergeyck, V., Cortvrindt, C., Bar, I., Eeckhout, Y., and Goffinet, A.M. (1999). Reelin, the extracellular matrix protein deficient in reeler mutant mice, is processed by a metalloproteinase. Exp. Neurol. *156*, 214–217.

Leahy, D.J., Dann, C.E., 3rd, Longo, P., Perman, B., and Ramyar, K.X. (2000). A mammalian expression vector for expression and purification of secreted proteins for structural studies. Protein Expr. Purif. *20*, 500–506.

Lee, D., Walsh, J.D., Mikhailenko, I., Yu, P., Migliorini, M., Wu, Y., Krueger, S., Curtis, J.E., Harris, B., Lockett, S., et al. (2006). RAP uses a histidine switch to regulate its interaction with LRP in the ER and Golgi. Mol. Cell *22*, 423–430.

Lo Conte, L., Chothia, C., and Janin, J. (1999). The atomic structure of protein-protein recognition sites. J. Mol. Biol. *285*, 2177–2198.

Lovell, S.C., Davis, I.W., Arendall, W.B., 3rd, de Bakker, P.I., Word, J.M., Prisant, M.G., Richardson, J.S., and Richardson, D.C. (2003). Structure validation by Calpha geometry: phi, psi and Cbeta deviation. Proteins *50*, 437–450.

Majeed, S., Ofek, G., Belachew, A., Huang, C.C., Zhou, T., and Kwong, P.D. (2003). Enhancing protein crystallization through precipitant synergy. Structure *11*, 1061–1070.

Miller, S., Janin, J., Lesk, A.M., and Chothia, C. (1987). Interior and surface of monomeric proteins. J. Mol. Biol. *196*, 641–656.

Murshudov, G.N., Vagin, A.A., and Dodson, E.J. (1997). Refinement of macromolecular structures by the maximum-likelihood method. Acta Crystallogr. D Biol. Crystallogr. *53*, 240–255.

Nielsen, K.L., Holtet, T.L., Etzerodt, M., Moestrup, S.K., Gliemann, J., Sottrup-Jensen, L., and Thogersen, H.C. (1996). Identification of residues in alpha-macroglobulins important for binding to the alpha2-macroglobulin receptor/Low density lipoprotein receptor-related protein. J. Biol. Chem. *271*, 12909–12912.

Nogi, T., Yasui, N., Hattori, M., Iwasaki, K., and Takagi, J. (2006). Structure of a signaling-competent reelin fragment revealed by X-ray crystallography and electron tomography. EMBO J. *25*, 3675–3683.

Nykjaer, A., and Willnow, T.E. (2002). The low-density lipoprotein receptor gene family: a cellular Swiss army knife? Trends Cell Biol. *12*, 273–280.

Otwinowski, Z., and Minor, W. (1997). Processing of X-ray diffraction data collected in oscillation mode. Methods Enzymol. *276*, 307–326.

Royer, W.E., Jr., Sharma, H., Strand, K., Knapp, J.E., and Bhyravbhatla, B. (2006). Lumbricus erythrocruorin at 3.5 A resolution: architecture of a megadalton respiratory complex. Structure *14*, 1167–1177.

Rudenko, G., Henry, L., Henderson, K., Ichtchenko, K., Brown, M.S., Goldstein, J.L., and Deisenhofer, J. (2002). Structure of the LDL receptor extracellular domain at endosomal pH. Science *298*, 2353–2358.

Sakai, J., Hoshino, A., Takahashi, S., Miura, Y., Ishii, H., Suzuki, H., Kawarabayasi, Y., and Yamamoto, T. (1994). Structure, chromosome location, and expression of the human very low density lipoprotein receptor gene. J. Biol. Chem. *269*, 2173–2182.

Sheldon, M., Rice, D.S., D'Arcangelo, G., Yoneshima, H., Nakajima, K., Mikoshiba, K., Howell, B.W., Cooper, J.A., Goldowitz, D., and Curran, T. (1997). Scrambler and yotari disrupt the disabled gene and produce a reeler-like phenotype in mice. Nature *389*, 730–733.

Stanley, P. (1989). Chinese hamster ovary cell mutants with multiple glycosylation defects for production of glycoproteins with minimal carbohydrate heterogeneity. Mol. Cell. Biol. *9*, 377–383.

 ©2010 Elsevier Ltd All rights reserved

Strickland, D.K., Gonias, S.L., and Argraves, W.S. (2002). Diverse roles for the LDL receptor family. Trends Endocrinol. Metab. *13*, 66–74.

Tissir, F., and Goffinet, A.M. (2003). Reelin and brain development. Nat. Rev. Neurosci. *4*, 496–505.

Trommsdorff, M., Gotthardt, M., Hiesberger, T., Shelton, J., Stockinger, W., Nimpf, J., Hammer, R.E., Richardson, J.A., and Herz, J. (1999). Reeler/Disabled-like disruption of neuronal migration in knockout mice lacking the VLDL receptor and ApoE receptor 2. Cell *97*, 689–701.

Utsunomiya-Tate, N., Kubo, K., Tate, S., Kainosho, M., Katayama, E., Nakajima, K., and Mikoshiba, K. (2000). Reelin molecules assemble together to form a large protein complex, which is inhibited by the function-blocking CR-50 antibody. Proc. Natl. Acad. Sci. USA *97*, 9729–9734.

Vagin, A., and Teplyakov, A. (1997). MOLREP: an automated program for molecular replacement. J. Appl. Crystallogr. *30*, 1022–1025.

Verdaguer, N., Fita, I., Reithmayer, M., Moser, R., and Blaas, D. (2004). X-ray structure of a minor group human rhinovirus bound to a fragment of its cellular receptor protein. Nat. Struct. Mol. Biol. *11*, 429–434.

Willnow, T.E., Hammes, A., and Eaton, S. (2007). Lipoproteins and their receptors in embryonic development: more than cholesterol clearance. Development *134*, 3239–3249.

Yamamoto, T., Davis, C.G., Brown, M.S., Schneider, W.J., Casey, M.L., Goldstein, J.L., and Russell, D.W. (1984). The human LDL receptor: a cysteine-rich protein with multiple Alu sequences in its mRNA. Cell *39*, 27–38.

Yasui, N., Nogi, T., Kitao, T., Nakano, Y., Hattori, M., and Takagi, J. (2007). Structure of a receptor-binding fragment of reelin and mutational analysis reveal a recognition mechanism similar to endocytic receptors. Proc. Natl. Acad. Sci. USA *104*, 9988–9993.